Supporting Information

Soft-Template-Carbonization Route to Highly Textured Mesoporous Carbon-TiO_2 Inverse Opals for Efficient Photocatalytic and Photoelectrochemical Applications

Li Na Quan,[a] Yoon Hee Jang,[ab] Kelsey A. Stoerzinger,[c] Kevin J. May,[b] Yu Jin Jang,[a] Saji Thomas Kochuveedu,[a] Yang Shao-Horn*[bc] and Dong Ha Kim*[ab]

[a]Department of Chemistry and Nano Science, Global Top 5 Research Program, Division of Molecular and Life Sciences, College of Natural Sciences, Ewha Womans University, 52, Ewhayeodae-gil, Seodaemun-gu, Seoul 120-750, Korea

[b]Department of Mechanical Engineering, Massachusetts Institute of Technology, 77 Massachusetts Ave, Cambridge, Massachusetts 02139, United States

[c]Department of Materials Science and Engineering, Massachusetts Institute of Technology, 77 Massachusetts Ave, Cambridge, Massachusetts 02139, United States

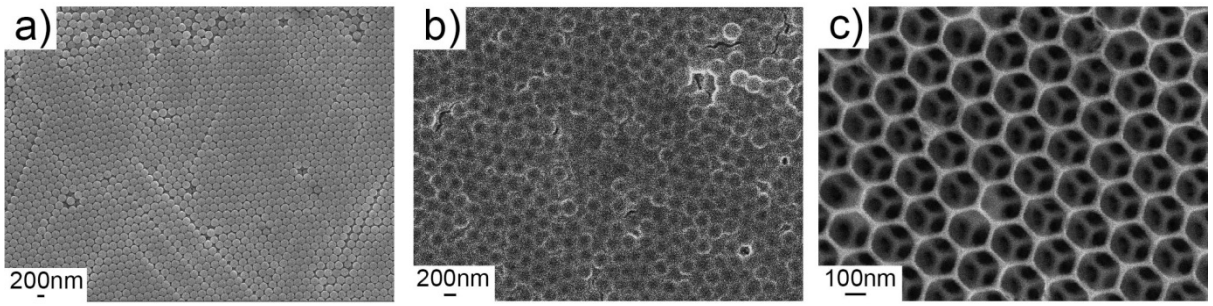

Figure S1. Field emission scanning electron microscopy (FESEM) images of a) PS colloidal nanoparticle arrays, b) PS template was infiltrated with the TiO_2 precursor solution, c) obtain ed neat-TiO_2 inverse opal.

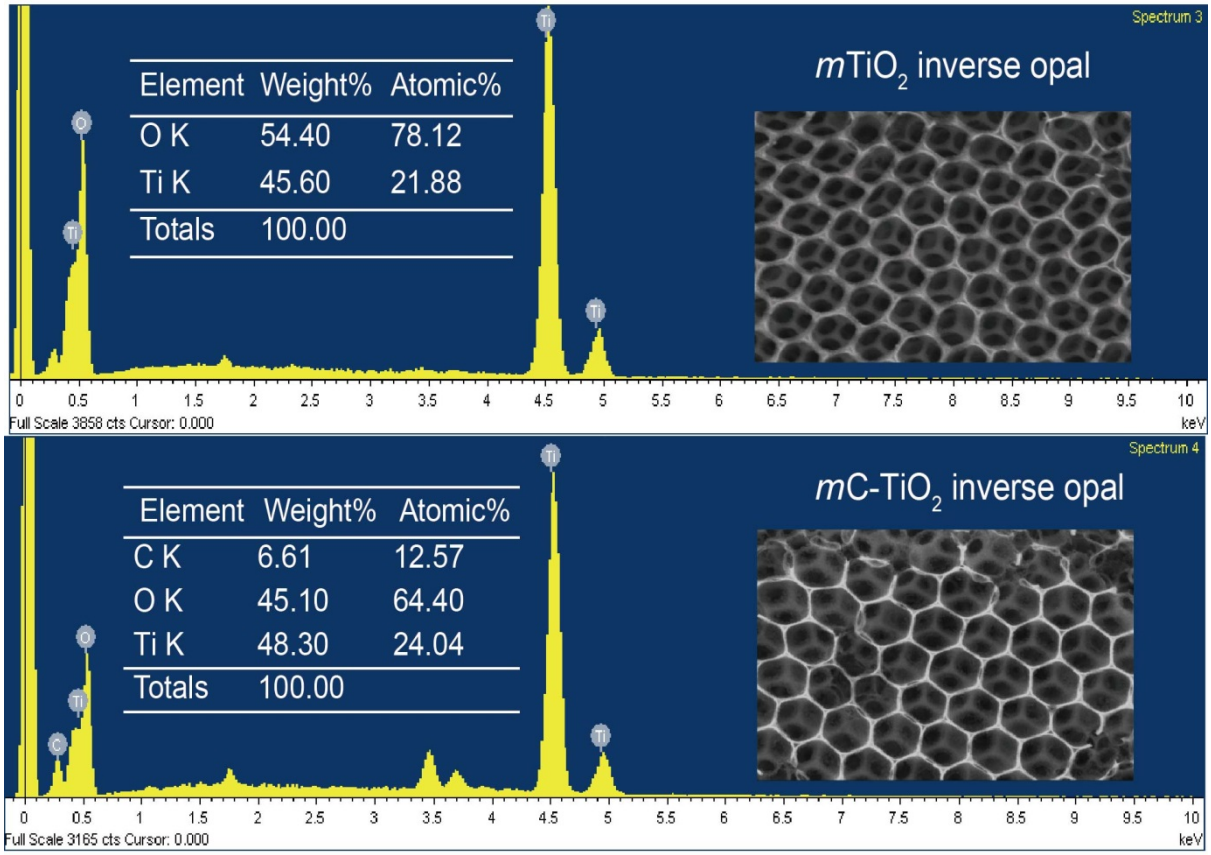

Figure S2. Energy-dispersive X-ray spectroscopy (EDX) results of *m*TiO_2 and *m*C-TiO_2 inverse opals.

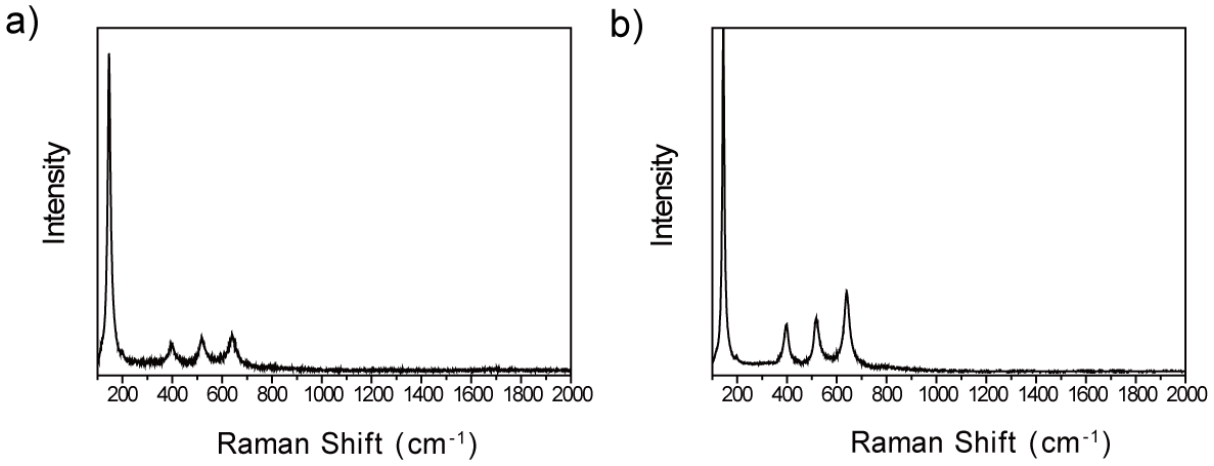

Figure S3. Raman spectra of a) neat TiO_2 and b) *m*TiO_2 inverse opals. The observed peaks at 144, 396, 515, 640 cm^{-1} are attributed to the characteristics of the anatase phase.

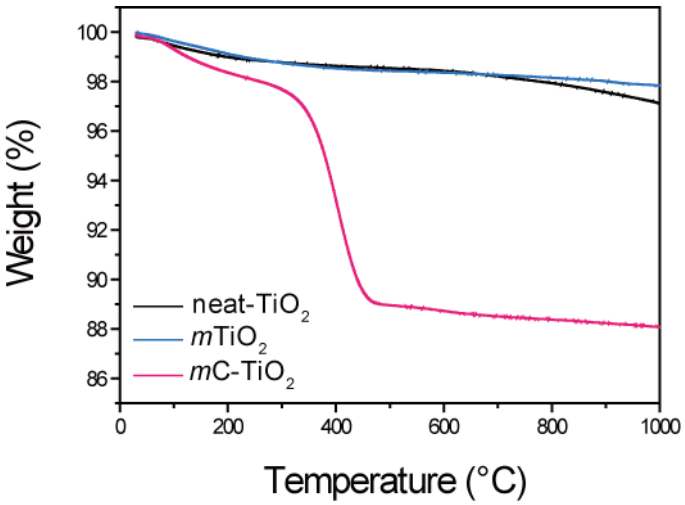

Figure S4. Thermogravimetric analysis (TGA) of neat TiO_2, *m*TiO_2 and *m*C-TiO_2 inverse opals.

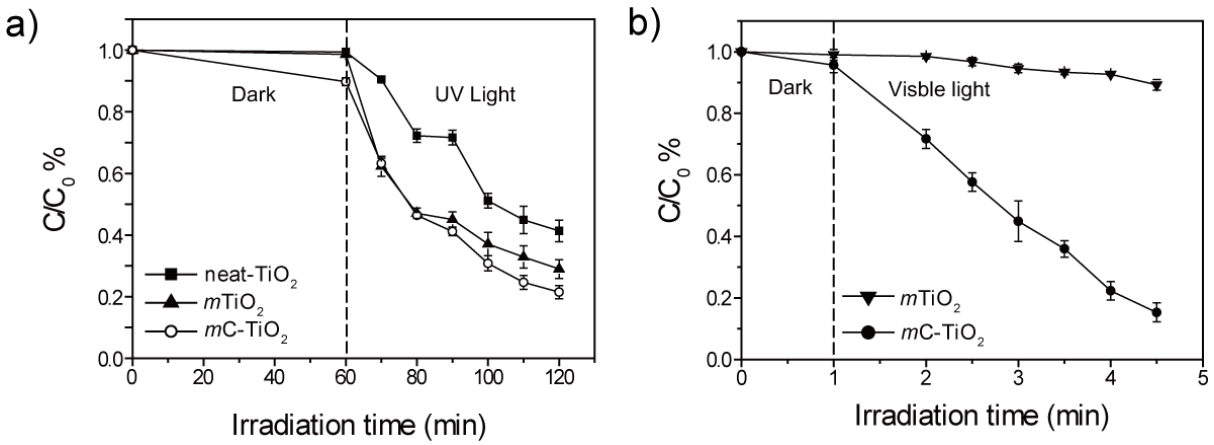

Figure S5. Plots of the concentration change of PNP versus reaction time in the presence of photocatalysts with error bars. a) neat TiO_2, *m*TiO_2 and *m*C-TiO_2 inverse opals under UV light irradiation, b) *m*TiO_2 and *m*C-TiO_2 inverse opals under visible light irradiation.

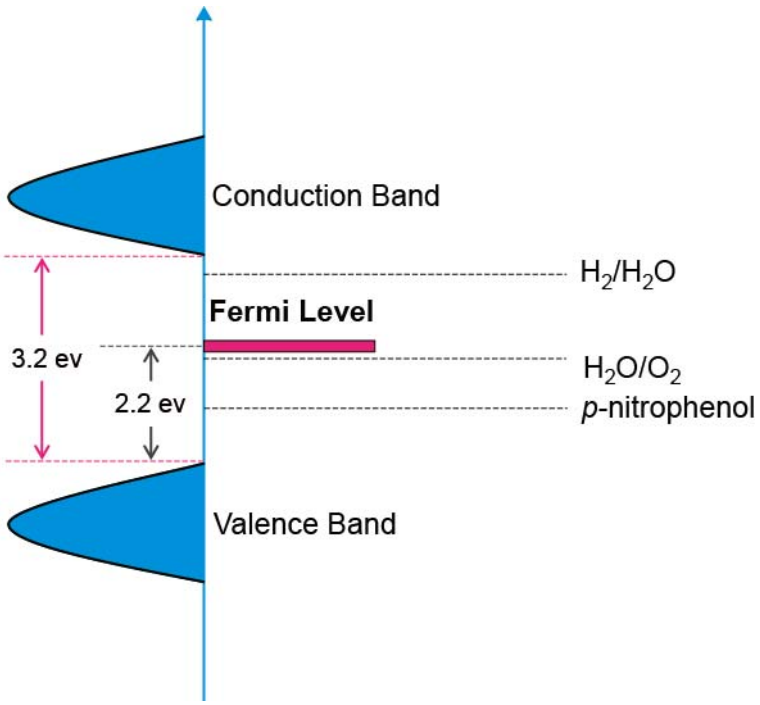

Figure S6. Relative energy band diagram of neat TiO_2 inverse opal.

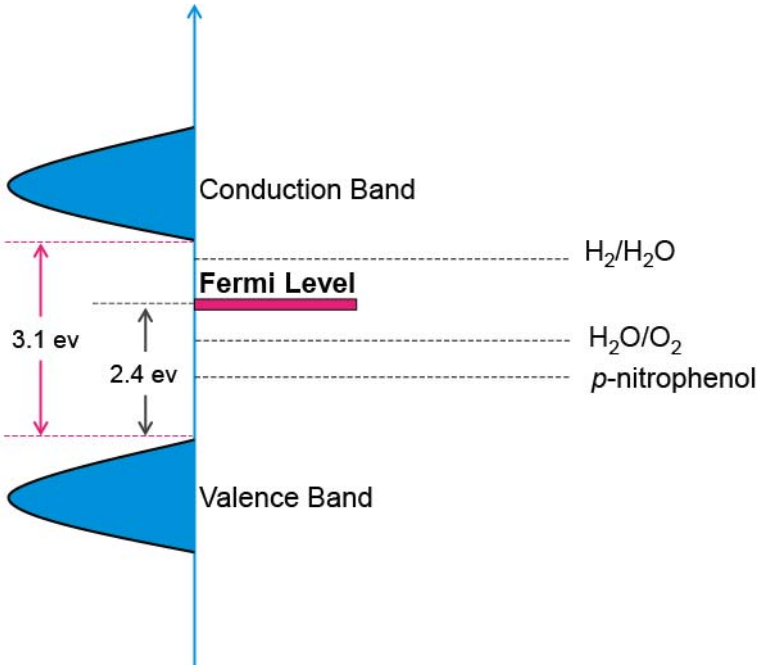

Figure S7. Relative energy band diagram of *m*TiO_2 inverse opal.